ORIGINAL ARTICLE

Metabolic insights into the yeast response to propionic acid based on high resolution ^{1}H NMR spectroscopy

Artur B. Lourenço · José R. Ascenso · Isabel Sá-Correia

Abstract The experimental model *Saccharomyces cerevisiae* has been widely used to elucidate the molecular mechanisms behind resistance to weak acids in fungi, an essential knowledge for the development of more suitable preservation strategies. Previous studies, based on transcriptomic and chemogenomic approaches, revealed a number of yeast responses to propionic acid, widely used in the preservation of bakery and fresh dairy products. In the present work we report the metabolic changes occurring during yeast adaptation to, and growth in, the presence of this weak acid (20 mM at pH 4) using high resolution ^{1}H NMR spectroscopy coupled with multivariate statistical analysis. The metabolic profiles highlighted the separation of propionic acid-induced lag-phase in two parts. The initial period of incubation under acid stress (up to 3 h following the inoculation of an unadapted yeast population) was characterized by a decrease of cell viability and of the average intracellular pH (pH_i) values. The final part of this incubation period (from 4 to 6 h of incubation) was characterized by the start of cell division in the presence of the acid, an increase of the average pH_i and a metabolic profile close to the profile exhibited by cells in the exponential phase of growth in propionic acid supplemented medium. An association between the average pH_i values and the levels of glutamate and propionate during growth latency was identified. Changes in the cell content in other amino acids, ATP, NAD$^+$, glycerol and trehalose were also registered during yeast incubation with propionic acid. These alterations are discussed in the context of the global response to this weak acid.

1 Introduction

Propionic acid is largely used in the preservation of bakery and fresh dairy products (Suhr and Nielsen 2004). Despite the presence of high concentrations of this and other weak acid food preservatives, like acetic, sorbic and benzoic acids, some spoilage yeasts are able to resume growth after an initial extended period of latency (Piper et al. 2001; Suhr and Nielsen 2004). The experimental model *Saccharomyces cerevisiae* has been widely used to elucidate the molecular mechanisms behind resistance to weak acids in fungi, an essential knowledge for the development of more suitable preservation strategies. The antimicrobial activity of weak acids at low pH relies on the effects of the undissociated acid form that may reach values close to the total concentration, depending on medium pH and the weak acid pKa (Piper et al. 2001; Suhr and Nielsen 2004). Undissociated forms of many weak acids are liposoluble and may stimulate the passive influx of H$^+$ into the cell by increasing plasma membrane non-specific permeability and affecting its biological function, in particular related with solute transport (Sá-Correia et al. 1989; Piper et al. 2001; Teixeira et al. 2007). Dissociation in the near-neutral cytoplasm of the permeant acid form leads to an additional

A. B. Lourenço · I. Sá-Correia (✉)
IBB—Institute for Biotechnology and Bioengineering, Centre for Biological and Chemical Engineering, Instituto Superior Técnico, Technical University of Lisbon, 1049-001 Lisbon, Portugal
e-mail: isacorreia@ist.utl.pt

J. R. Ascenso
Centro de Química Estrutural, Instituto Superior Técnico, Technical University of Lisbon, 1049-001 Lisbon, Portugal

acidification of the cell interior (Piper et al. 2001; Suhr and Nielsen 2004). The cell ability to grow or maintain viability at a high weak acid concentration may reflect their capacity to maintain control over their internal pH. Indeed, the proper functioning of yeast cells relies on maintenance of their pH_i within relatively narrow limits, as large deviations from the normal pH severely inhibit metabolism as a result of suboptimal activities of cytosolic enzymes (Holyoak et al. 1996; Piper et al. 2001). Additionally, the maintenance of the electrochemical potential of plasma membrane is crucial to the secondary active uptake of nutrients across the plasma membrane and for detoxification. Since under glucose-repression, *S. cerevisiae* is unable to catabolize propionate (Pronk et al. 1994) and propionate is unable to readily diffuse out of the cell, this counter ion tends to accumulate intracellularly. However, it was proposed that adapted cells are able to actively expulse propionate through plasma membrane transporters, in particular through the action of Pdr12p (Piper et al. 1998) belonging to the ATP-Binding Cassette (ABC) Superfamily. Pdr12p was identified as being up-regulated ($3.5\times$) during the early response to propionic acid and to be required for maximal resistance this weak acid (Mira et al. 2009). The expression of a number of genes encoding drug:H^+ antiporters belonging to the Major Facilitator Superfamily (MFS) are also required for maximal tolerance to propionic acid, presumably by reducing the intracellular concentration of the counter-ion, either directly, by promoting its extrusion, or indirectly, by affecting the partition of the weak acid between the exterior and the intracellular environment through the alteration of intracellular pH (pH_i) and/or plasma membrane potential (Sá-Correia et al. 2009). Transcriptomic and chemogenomic analyses allowed the characterization of the early yeast transcriptomic response to propionic acid and the identification of genes required for maximal tolerance to propionic acid (Mira et al. 2009). Under propionic-acid-induced stress, the up-regulation of a number of genes encoding glycolytic enzymes was registered (Mira et al. 2009, 2010), presumably to compensate the severe depletion of ATP registered in these stressed cells (Holyoak et al. 1996; Krebs et al. 1983). The up-regulation of genes encoding proteins involved in the uptake and biosynthesis of amino acids in propionic acid-stressed cells was also registered (Mira et al. 2009, 2010). The clustering of the set of genes required for maximal tolerance to propionic acid revealed the enrichment of genes involved in "intracellular trafficking", "protein catabolism through the multivesicular body (MVB) system", "generation of ATP and energy", "ergosterol biosynthesis", "regulation of pH_i" and "vacuolar function" (Mira et al. 2009).

To get additional insights into the yeast response to propionic acid and giving that metabolites can be regarded as the ultimate response of biological systems to an environmental change (Fiehn 2002), a metabolomic analysis was undertook. Results of the exploration of ^{1}H-NMR-based-metabolomics coupled with multivariate statistical analysis allowed the characterization of the changes occurring in the yeast metabolome during adaptation to, and growth in, the presence of propionic acid. The metabolic profiles obtained were confronted with the concentration of viable cells and the average pH_i of the yeast population during the growth curve in propionic acid supplemented medium.

2 Materials and methods

2.1 Strains, growth media and growth conditions

Saccharomyces cerevisiae BY4741 (*MAT**a**, his3Δ1, leu2Δ0, met15Δ0, ura3Δ0*), obtained from the Euroscarf collection, was used in this work. Cells were batch-cultured at 30°C, with orbital agitation (250 rpm) in minimal growth medium MM4, acidified with HCl to pH 4.0. This medium contained (per liter): 1.7 g yeast nitrogen base without amino acids or NH_4^+ (Difco), 20 g glucose (Merck), 2.65 g $(NH_4)_2SO_4$ (Merck), 20 mg methionine (Merck), 20 mg histidine (Merck), 60 mg leucine (Sigma) and 20 mg uracil (Sigma). To examine the effect of propionic acid, MM4 medium was supplemented with 20 mM of this acid (Sigma-Aldrich) adjusted to pH 4.0. Growth curves were followed by measuring culture optical density (OD_{600nm}). The concentration of viable cells was assessed as the number of colony-forming units (CFU) onto YPD solid medium, following incubation for 3 days at 30°C. YPD solid medium contained (per liter): 20 g glucose, 20 g Yeast Extract (Difco), 10 g BactoPeptone (Difco) and 20 g of Agar (IberAgar). Cells used to prepare the inocula were cultivated in the absence of propionic acid until mid-exponential phase at a standardized $OD_{600nm} = 0.5 \pm 0.01$. These cells were used to inoculate the different media to obtain an initial $OD_{600nm} = 0.2 \pm 0.01$.

2.2 Assessment of intracellular pH

Intracellular pH values were assessed by fluorescence microscopy using the pH-sensing fluorescent probe 5-(and 6-)carboxyfluorescein diacetate, succinimidylester [5(6)-CFDA, SE]. This technique makes use of a membrane-permeant fluorescent probe that accumulates intracellularly and undergoes pH-dependent changes, in both its absorption and its fluorescence emission spectra in a wide range of pH values (Roberts et al. 1991). This property has been exploited to assess yeast pH_i (Viegas et al. 1998; Vindelov and Arneborg 2002; Fernandes et al. 2003). Briefly, yeast

cells were harvested by filtration, washed twice with CF buffer (50 mM glycine, 10 mM NaCl, 5 mM KCl and 1 mM MgCl$_2$ in 40 mM Tris—100 mM MES, pH 4.0) and resuspended in 2 ml of CF buffer to an OD$_{600}$ nm of 10. The probe 5(6)-CFDA, SE was added to the cell suspension (final concentration of 40 mM) and the mixture was vortexed in one burst of 10 s and incubated for 20 min at 30°C with orbital agitation (250 rpm). After fluorescent labelling, cells were centrifuged at 5,500×g for 5 min (at 4°C), washed twice with CF buffer and finally resuspended in 2 ml of the same buffer. Cells were immediately examined with a Zeiss Axioplan microscope equipped with epifluorescence interference filter (Zeiss BP450-490). Fluorescence emission was collected with a cooled CCD camera (Cool SNAPFX, Roper Scientific Photometrics). Brightfield images for pH$_i$ determination were obtained concurrently and recorded at 1-min intervals, each experiment being completed within 15 min. The images were analyzed using METAMORPH 3.5, and fluorescence images were background corrected using dark-current images. In each experiment, at least 1,000 individual cells were examined and the value of fluorescence intensity emitted by each cell was obtained pixel by pixel in the region of interest to estimate pH$_i$. The conversion of fluorescence intensity signals of 5(6)-CFDA, SE into pH$_i$ values was performed based on an in vivo calibration curve using cell a suspension grown in the absence of acid. Cells were loaded with the fluorescent probe as described above and incubated for 30 min with 0.5 mM carbonyl cyanide m-chlorophenylhydrazone to dissipate the plasma membrane pH gradient. Then, the external pH was adjusted (in the range 3.5–6.8) by the addition of HCl or NaOH. The average pH$_i$ values presented are means of three independent experiments.

2.3 Metabolome profiling

2.3.1 Cell sampling, cold methanol quenching and metabolite extraction

Cell samples were collected at times, 5 and 45 min, and 2, 3, 4, 5, 6 and 12 h after inoculation of the fresh medium supplemented with 20 mM of propionic acid. Cell samples were also collected after 5 min of incubation in unsupplemented medium and when the cell culture reached an OD$_{600nm}$ = 0.5 ± 0.01 in unsupplemented medium. In order to capture snapshots as accurate as possible of the metabolome, cell metabolism was quenched using a previously described method (de Koning and Van Dam 1992). One volume of cell culture (approximately 30 mg dry weight) was immediately added in three volumes of methanol cold solution (60% v/v; T < −50°C). Cells were pelleted in a centrifuge cooled to −20°C (2,500×g for 6 min). Pellets were washed three times. Eight ml of the

methanol cold solution were added to the pellets, vortexed, and pelleted again in a centrifuge cooled to −20°C (2,500×g for 3 min). After each centrifugation step, samples were checked for their temperature using a thermometer (−35°C to +50°C). During cold methanol quenching and subsequent washing steps, the temperature of the mixture was always well below −20°C. Metabolites were extracted based on the method described by Gonzalez et al. (1997). Two ml of glass beads (0.4–0.6 mm diameter) and 4 ml of ethanol (75% v/v) were added to the cell pellets, the mixture was then vortexed for 30 s, heated for 3 min to 80°C and vortexed again for 30 s. The supernatant was decanted and the extraction step repeated a second time with 2 ml of ethanol (75% v/v). The supernatants were mixed, cleared by centrifugation (−20°C; 16,000×g; 10 min) and dried under vacuum.

2.3.2 NMR data acquisition, processing and resonance assignments

The dried extracts were dissolved in 0.8 ml of buffer (0.2 M phosphate buffer pH 6.85, in D$_2$O, containing 0.3 mM of trimethylsilyl-2,2,3,3-tetradeuteropropionate (d$_4$-TSP)) and filtrated (0.22 μm filters) into 5 mm diameter NMR tubes. The samples were analysed using a 500 MHz Avance III Bruker spectrometer, equiped with a 5 mm inverse probe (TXI), at 296 K. 1D proton spectra were acquired at constant gain, with 1,024 transients and a spectral width of 12 ppm. A train of Carr-Purcell-Meiboom-Gill (CPMG) echoes, of 40 ms long, was used to reduce macromolecules broad signals. The residual water peak was presaturated during the relaxation delay of 2 s. All proton spectra were manually phased, baseline corrected and referenced to d$_4$-TSP (δ 0.00 ppm) using the program Mnova v5.3 for NMR data processing. For metabolite identification purpose 2D J-resolved (128 × 8 K data points, relaxation delay of 2 s, 128 transients per FID and a spectral width of 62.5 Hz in the 2nd dimension), Total Correlation Spectroscopy (TOCSY; 512 × 2 K data points, relaxation delay of 2 s, mixing time of 60 ms and 64 transients per FID) and Heteronuclear Single Quantum Coherence (HSQC; 512 × 2 K data points, relaxation delay of 1.5 s, 64 transients per FID and a spectral width of 158.7 Hz in indirect dimension) spectra were collected for representative samples. The identity of the metabolites was confirmed by spiking samples with authentic standards.

2.3.3 Multivariate data analysis

Spectra regions corresponding to residual water and ethanol were excluded (5.15–4.50, 3.73–3.63 and 1.26–1.14 ppm). When comparing proton spectra from extracts prepared

from cells grown in the presence or in the absence of propionic acid, the regions corresponding to propionate were also excluded. To account for mass differences between samples, all proton spectra were normalized to the total intensity between 9.50 and 0.70 ppm. Each spectrum was integrated over a series of fixed width bins (0.005 ppm) using Mnova v5.3 features. All spectra were put in a data table form, where each row is a spectrum and each column is a bin, in an ASCI format file. This file was imported into the software SIMCA-P12$^+$ for multivariate data analysis. In SIMCA-P12$^+$ the data was pre-processed using Pareto scaling. Data was analyzed using Principal Component Analysis (PCA) and Orthogonal Projection on Latent Structures Discriminant Analysis (O-PLS-DA). These methods are used for modeling complex data, while reducing the dimensionality of the problem to a small set of latent variables (principal components). Unsupervised methods like PCA give an overview of the data and clusters the observations, while supervised methods based on prior information are used to better discriminate between clusters. R^2 and Q^2 values were considered as measures of goodness of model and the model robustness, respectively. R^2 is the fraction of variance explained by a component, and cross validation of this component provides Q^2 which describes the fraction of the total variation predicted by a component. The value of Q^2 ranges from 0 to 1 and typically a Q^2 value of greater than 0.4 is considered a good model, and those with Q^2 values over 0.7 are robust. Interpretation of each supervised model was based on the scores plot, the loadings plot and the variables importance in the projection plot (VIP). Variables lying in the same region in the loadings plot as to the observations in the scores plot are enriched in those observations. A measure of the degree to which a particular variable explains cluster membership is obtained with the VIP plot (with confidence intervals derived from jack knifing routine). For a given variable a VIP value above 1 indicates that it is important for class membership. Data corresponding to propionic acid-induced lag phase were assessed by O-PLS that regress an external variable against metabolic profile.

3 Results

3.1 Inhibition of yeast growth curve by propionic acid

The growth curves of *Saccharomyces cerevisiae* BY4741 in MM4 medium either or not supplemented with 20 mM of propionic acid (at pH 4.0; initial culture OD$_{600nm}$ of 0.2), show that the sudden exposure of an unadapted yeast cell population to weak acid supplemented medium leads to a lag-phase of approximately 6 h (Fig. 1A). During this adaptation period, the culture OD$_{600nm}$ remains almost

constant while the profile of the viable cells concentration indicates a slight loss of viability of the initial cell population during the first 3–4 h of incubation under propionic acid stress (Fig. 1B). After this early adaptation period, part of the cells of the heterogeneous initial population (Viegas et al. 1998), start to divide (from 4 to 6 h of incubation), followed by the resumption of the exponential growth by the whole viable population (Fig. 1B). This adapted cell population exhibited an inhibited maximum specific growth rate due to the presence of the acid (Fig. 1).

3.2 Intracellular pH profile during propionic acid stressed cultivation

The alteration of pH$_i$ during yeast cultivation in the presence of 20 mM propionic acid was monitored by using a fluorescence microscopic image processing. This experimental approach allowed a clear-cut picture of the pH$_i$ of
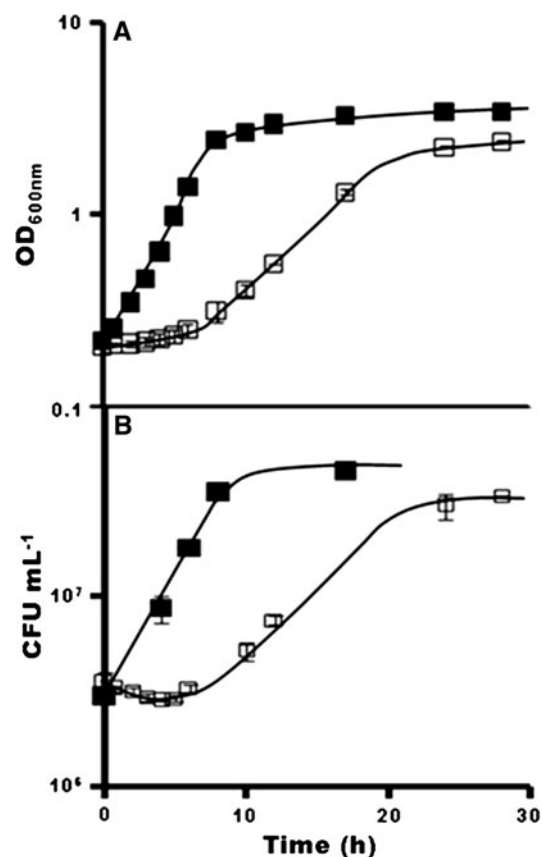

Fig. 1 Growth curves of *Saccharomyces cerevisiae* BY4741 in MM4 (pH 4.0) (*filled square*) or in this same basal medium supplemented with 20 mM propionic acid (pH 4.0) (*open square*). Growth was followed by measuring culture OD$_{600nm}$ (**A**) and the concentration of viable cells (**B**), assessed as the number of Colony Forming Units per milliliter of cell culture (CFU ml^{-1})

Fig. 2 Average pH_i of the whole cell population (**A**); percentage of yeast cells with pH_i below 5.5 (**B**), between 5.5 and 6.0 (**C**), or above 6.0 (**D**) during *S. cerevisiae* BY4741 cultivation at 30°C in medium supplemented with 20 mM total propionic acid (pH 4.0) (*filled square*). The average pH_i values estimated for the whole cell population are the arithmetical mean values of the various average pH_i values calculated for individual cells. The percentage of cells with pH_i values within the three ranges (**B**, **C** and **D**) is shown and the average pH_i after 5 min of incubation in fresh medium in the absence of propionic acid is also indicated (*open square*). Results are the means of three independent experiments
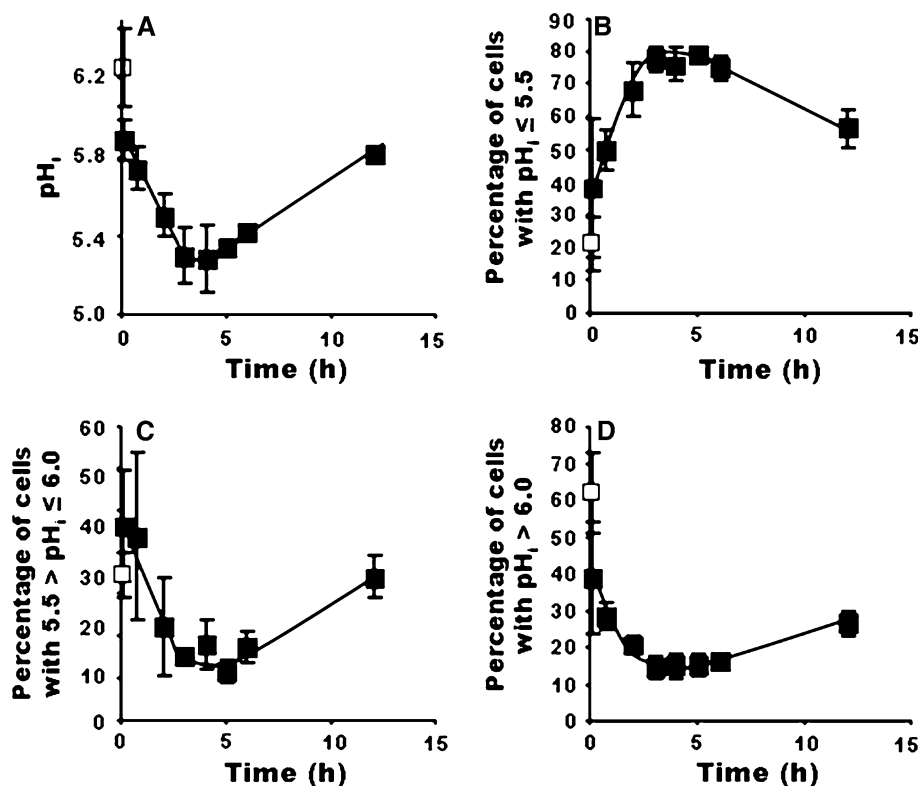
individual cells, giving information about the distribution of pH_i values of a yeast cell population (Fig. 2), instead of solely an estimation of the average value of the whole population, as it is the case with techniques based on the distribution of radioactive propionic acid (Viegas and Sá-Correia 1995) or on the in vivo ^{31}P nuclear magnetic resonance (Carmelo et al. 1997). Sudden exposure of the initial cell population to propionic acid was found to induce a decrease of the average pH_i to 5.9 ± 0.10 after 5 min of incubation in propionic acid supplemented medium compared to an average pH_i of 6.3 ± 0.20 after 5 min incubation in propionic acid free-medium. This propionic acid-induced decrease of the average pH_i resulted from a significant increase of the percentage of the cell population with a pH_i below 5.5. During the first 3 h of incubation with propionic acid, the percentage of the yeast population with a pH_i below 5.5 continued to increase, reaching nearly 80% of the cell population, while the percentage of the cell population with a pH_i in the range 5.5–6.0, and above 6.0 suffered a corresponding decrease (Fig. 2). During exponential growth in the presence of propionic acid, the pH_i recovered up to more physiological levels, reaching an average pH_i of 5.8 ± 0.02 (Fig. 2).

3.3 Identification of intracellular metabolites

The analysis of the ^{1}H NMR spectra acquired from cell extracts prepared from yeast cells grown either in the presence or absence of propionic acid enabled the detection of over 30 metabolites (Fig. 3). Metabolite assignment was done by a careful analysis of chemical shifts, intensities, J couplings and multiplicities of the metabolites peaks present in the 1D proton spectra, complemented with the information from J-resolved, TOCSY and HSQC spectra, and from different databases (Lundberg et al. 2005; Cui et al. 2008; Wishart et al. 2009). All the assigned metabolites, with the exception of asparagine, were confirmed by spiking with authentic standards. Although several peaks remained unassigned, a wide range of classes of biomolecules were identified, including amino acids (alanine, valine, arginine, histidine, aspartate, glutamate and glutamine), cofactors (NAD^+ and $NADP^+$), osmolytes (glycerol and trehalose), and metabolites associated with energy metabolism (ATP and AMP).

3.4 Metabolite dynamics during yeast cultivation in the presence of propionic acid

The dynamics of the relative abundance of several metabolites during yeast cultivation in medium supplemented with propionic acid are summarized in Fig. 4. PCA of all the collected data during yeast cultivation in the presence of propionic acid ($R^2X = 0.862$ and $Q^2 = 0.735$) revealed some interesting features (Fig. 5). The metabolic profiles of cells harvested following 5 and 45 min, 2 and 3 h of incubation cluster together and are clearly distinct
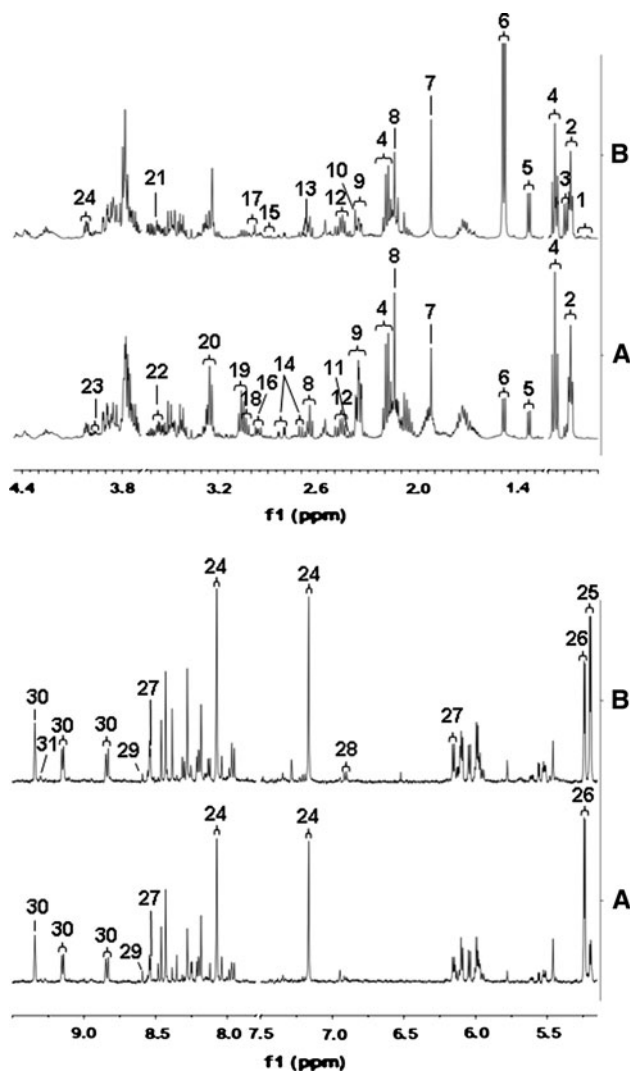
Fig. 3 High-resolution ^{1}H NMR spectrum of a typical extract from cells of *Saccharomyces cerevisiae* BY4741 harvested after 5 min (**A**) or during 12 h (**B**) of incubation in the presence of propionic acid. Key: *1* 2-isopropylmalate, *2* leucine, *3* valine, *4* propionate, *5* threonine, *6* alanine, *7* acetate, *8* methionine, *9* glutamate, *10* pyruvate, *11* succinate, *12* glutamine, *13* citrate, *14* aspartate, *15* asparagine, *16* reduced glutathione, *17* oxidized glutathione, *18* lysine, *19* ornithine, *20* arginine, *21* glycine, *22* glycerol, *23* serine, *24* histidine, *25* trehalose, *26* glucose, *27* ATP, *28* tyrosine, *29* AMP, *30* NAD, *31* NADP

from those obtained from cells harvested following 4, 5 and 6 h of incubation (Fig. 5C). Indeed, the metabolic profiles separate between an initial part (up to 3 h of incubation) and a final part (until 6 h of incubation) of the propionic acid-induced lag-phase. Cells harvested during the final part of the lag-phase are metabolically closer to cells harvested during the propionic acid-adapted exponential growth phase (harvested after 12 h of incubation) than to the cells harvested during the initial part of the lag-phase. These metabolic features are consistent with the viable cell concentration profile, since the initial part of the propionic

acid-induced lag-phase is characterized by a slight loss of cell viability, while during the final part, cell division was resumed. The analysis of the metabolic profiles also indicates that during the initial part of the lag-phase there is a more evident metabolic dynamics than during the final part of the lag-phase, since consecutive time points during the initial part are more clearly distinguishable among themselves than consecutive time points during the final part of the lag-phase.

The regression of either incubation time or average cell pH_i against the metabolic profile evidenced the general trends of the alteration of the relative abundance of some metabolites during the propionic acid-induced lag-phase. Although this approach poorly describes features in X (metabolic profiles) that do not align with the external variable, O-PLS was very useful to relate metabolic features with an external variable (Westerhuis et al. 1999). Regression of incubation time against metabolic profile (O-PLS model with $R^2X = 0.615$; $R^2Y = 0.960$; $Q^2 = 0.940$) evidenced that during the acid-induced lag-phase there is a decrease in the relative abundance of the amino acids arginine, ornithine and lysine, and also of glucose. The overall trend indicates an increased abundance of the amino acids alanine, valine, glycine and threonine, and of the metabolites trehalose and glycerol during acid-induced lag-phase. PCA loadings plot (Fig. 5B) allowed the identification of positive or negative correlations between different metabolites. Metabolite-to-metabolite correlation analysis revealed the existence of correlations between arginine and ornithine ($R^2 = 0.629$; $R = 0.793$; Significance F $= 4.820 \times 10^{-7}$), arginine and lysine ($R^2 = 0.455$; $R = 0.674$; Significance F $= 8.318 \times 10^{-5}$) and between leucine and methionine ($R^2 = 0.956$; $R = 0.978$; Significance F $= 3.414 \times 10^{-19}$). In this metabolite-to-metabolite correlation analysis all time points during the acid-induced lag-phase were used for the estimation of correlation parameters, which is probably an oversimplification of the time-course nature of the data but still very useful as an indication of the correlation between the relative abundances of two metabolites. Regression analysis revealed the existence of a correlation between threonine and glycine ($R^2 = 0.785$; $R = 0.886$; Significance F $= 3.625 \times 10^{-10}$) and between alanine and valine ($R^2 = 0.894$; $R = 0.946$; Significance F $= 3.437 \times 10^{-14}$). Regression of the average pH_i against metabolic profile (O-PLS model with $R^2X = 0.737$; $R^2Y = 0.960$; $R^2Y = 0.980$; $Q^2 = 0.955$) evidenced the relation between pH_i and both glutamate and propionate. During the initial part of the propionic acid-induced lag-phase, a decrease in pH_i is accompanied by a decrease in the abundance of glutamate and an increase in the abundance of propionate, while when the pH_i increases during the final part of the acid-
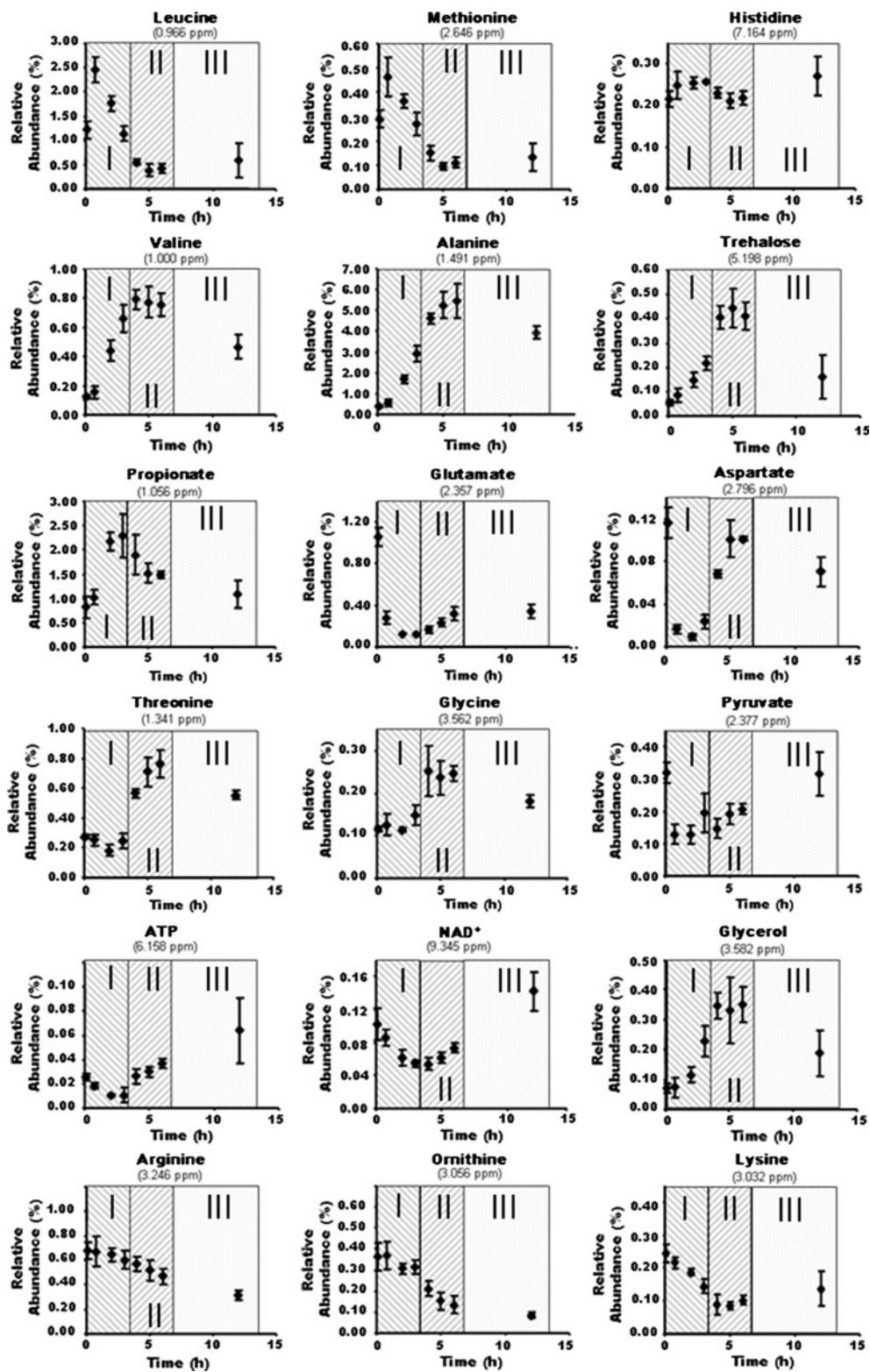
Fig. 4 Variation in the relative abundance of selected metabolites during cultivation of *Saccharomyces cerevisiae* BY4741 in growth medium supplemented with propionic acid. Each *plot* displays the variation in the relative abundance of a representative bin for each metabolite in the spectrum. Experimental values are means of four independent experiments with standard deviation *error bars*. Three different phases can be defined during the growth curve in the presence of propionic acid. *Key*: *I* corresponding to the initial part of the acid-induced lag-phase characterized by a slight loss of cell viability, *II* corresponding to the final part of the acid-induced lag-phase during which part of the cell population resume cell division, *III* corresponding to the exponential growth phase of the whole cell population
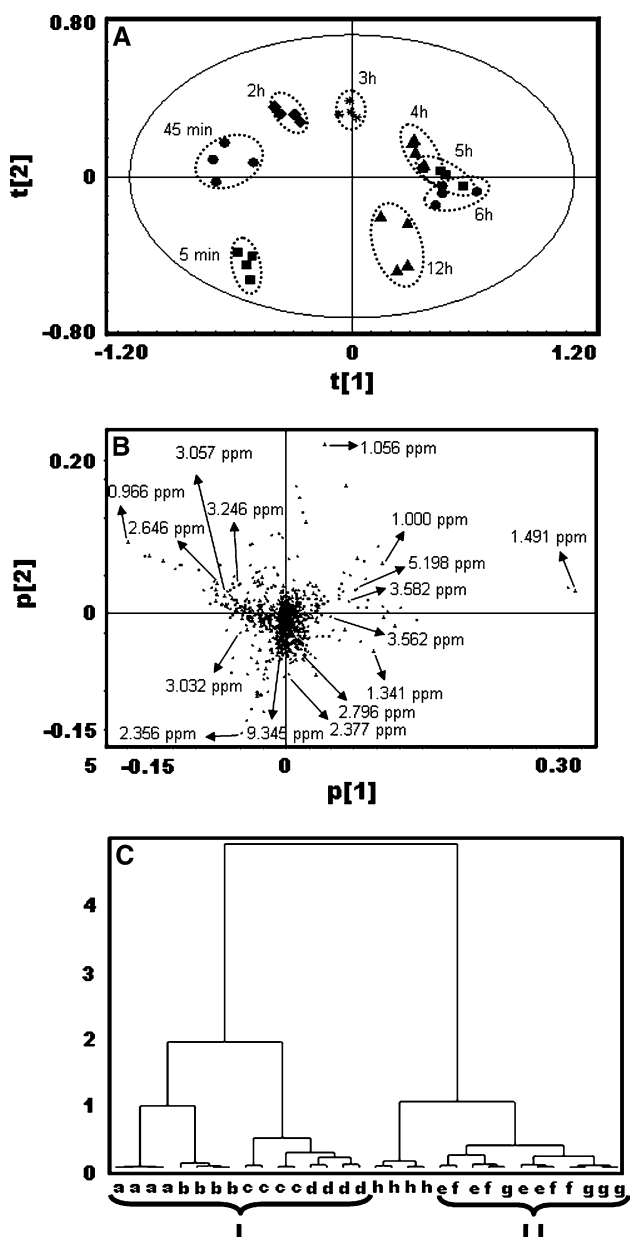
Fig. 5 Analysis of extracts from yeast cells cultivated in growth medium supplemented with propionic acid using ^{1}H NMR spectroscopy and PCA. (A) 2D scores plot displaying the space formed by the two first principal components (R^2X for PC1 equal to 0.466 and R^2X for PC2 equal to 0.192), (B) 2D loadings plot displaying the space formed by the two first principal components and (C) dendrogram based on the PCA scores (ward clustering distance measure) considering all six principal components. Key: *a* 5 min, *b* 45 min, *c* 2 h, *d* 3 h, *e* 4 h, *f* 5 h, *g* 6 h and *h* 12 h; *I* corresponding to the initial part of the acid-induced lag-phase characterized by a slight loss of cell viability, *II* corresponding to the final part of the acid-induced lag-phase during which part of the cell population resume cell division

induced lag-phase there is an increase in the abundance of glutamate and a decrease in the abundance of propionate (Figs. 2, 4). Regression analysis revealed the existence of a correlation between propionate and glutamate during

acid-induced lag-phase ($R^2 = 0.465$; $R = -0.682$; Significance $F = 6.433 \times 10^{-5}$). The acidic amino acid aspartate exhibits a dynamics similar to glutamate ($R^2 = 0.412$; $R = 0.642$; Significance $F = 4.042 \times 10^{-4}$), especially during the initial part of the acid-induced lag-phase, but its values recovered much faster than the glutamate values during the final part of the propionic acid-induced lag-phase (Fig. 4).

3.5 Metabolic response to the presence of propionic acid

3.5.1 Metabolic changes in yeast cells suddenly exposed to propionic acid

To study the effect that propionic acid has in the metabolome of yeast cells suddenly exposed to the acid, the metabolic profiles of yeast cells harvested after 5 min of incubation in medium either or not supplemented with 20 mM of propionic acid were compared. An initial analysis by PCA ($R^2X = 0.769$ and $Q^2 = 0.685$) indicated a clear distinction between yeast cells suddenly exposed to propionic acid and non-stressed cells. The O-PLS-DA for this two-way comparison ($R^2X = 0.934$, $R^2Y = 1.000$ and $Q^2 = 0.987$) show that yeast cells sudden exposed to propionic acid have a higher relative abundance of pyruvate and succinate, and also of the amino acids alanine, valine, leucine, methionine, glutamate and glutamine (Table 1). On the other hand, among other metabolites, ATP and the amino acids lysine, arginine and ornithine displayed decreased relative abundances (Table 1).

3.5.2 Metabolic differences between exponentially growing cells in the presence or absence of propionic acid

To study the effect that propionic acid has in the metabolome of yeast cells during the exponential phase of growth, the metabolic profiles of exponentially growing cells either in the presence or absence of propionic acid were compared. The analysis of the extracts obtained from non-stressed cells (in mid-exponential phase at an OD_{600nm} of 0.5) and from propionic acid-adapted cells in the exponential growth phase (after 12 h of incubation in propionic acid supplemented medium) shows that they are clearly different (PCA model with $R^2X = 0.676$ and $Q^2 = 0.558$). The O-PLS-DA modeling of the data ($R^2X = 0.676$, $R^2Y = 0.990$ and $Q^2 = 0.978$) identified several amino acids responsible for this separation (Table 1). Specifically, propionic acid-adapted cells exhibit a higher abundance of the amino acids alanine and valine, while non-stressed cells exhibit a higher abundance of arginine, lysine and ornithine.

Table 1 Summary of the metabolic differences detected when yeast cells cultivated for 5 min or during exponential growth (after 12 h of incubation) in the presence of propionic acid were compared with yeast cells cultivated for 5 min or during exponential growth in the same growth medium in the absence of the acid, respectively

Growth conditions	Metabolites showing an increase in their relative abundance in cells cultivated in the presence of propionic acid	Metabolites showing an decrease in their relative abundance in cells cultivated in the presence of propionic acid
After 5 min of incubation	Leucine, methionine, alanine, valine, succinate, pyruvate, glutamate, aspartate, glutamine, threonine,	ATP, NAD^+, acetate, glycerol, arginine, ornithine, lysine
During exponential growth	Alanine, valine, glutamine, threonine	Arginine, ornithine, lysine, glutamate

4 Discussion

Saccharomyces cerevisiae has evolved to respond rapidly and effectively to the alteration of environmental conditions, in particular to respond to sudden exposure to stress. In this study, propionic acid acute stress was found to cause an early change in the yeast metabolome and, in the long term, to induce metabolic modifications to reestablish homeostasis in a new homeostatic state. The dynamics of the pools of metabolites during adaptation to, and growth in the presence of, propionic acid provided useful insights into metabolome remodeling in response to this weak acid induced stress.

During the initial part of growth latency following the inoculation of an unadapted yeast cell population into propionic acid-supplemented medium, the viability of the cell population decreased accompanying intracellular acidification, as described before for other weak acids (Imai and Ohno 1995; Viegas et al. 1998). The metabolic profiles revealed a clear separation between the initial part of the early response to propionic acid and the final part of the acid-induced lag-phase. During this final period cell duplication is resumed by part of the heterogeneous cell population present in the inoculum (Viegas et al. 1998) and the average pH_i starts to recover to more physiological values. The metabolic data also suggest the existence of an association between the whole cell population average pH_i and the relative abundance of both propionate and glutamate. Acidic amino acids, like glutamate and aspartate are located almost exclusively in the cytosol (Klionsky et al. 1990). In order to maintain electrical neutrality, the accumulation of acetate in *Escherichia coli* during acetic acid stress is compensated by an exchange of physiological anions, being the decrease of glutamate a major compensatory mechanism (Roe et al. 1995). Our results suggest that, in *S. cerevisiae*, a similar mechanism may occur, whereas the loss of glutamate during the early response to propionic acid stress compensates, at least partially, propionate accumulation in the cell interior. This mechanism is consistent with previous transcriptomic data, showing that during the early response to propionic acid the genes involved in glutamate degradation (*GAD1*, *UGA1* and *UGA2*) are up-regulated (Mira et al. 2009) (Fig. 6).

The cell content in other amino acids also showed a complex and dynamic profile during incubation in the presence of propionic acid. Following yeast cells inoculation into propionic acid supplemented medium, an increase in the intracellular abundance of leucine and methionine and a slight increase in histidine was registered. These three amino acids were added in the growth medium due to the yeast strain auxotrophies. The relative abundance of leucine and methionine peaked after 45 min of incubation and suffered a decrease through the rest of the lag-phase period, reaching identical levels in acid-adapted and in non-stressed cells during exponential growth. Although there are no results for the exo-metabolome profile, since the yeast strain used in this work is unable to synthesize methionine, leucine and histidine, the time course evolution of these amino acids during the early response to propionic acid stress is likely attributed to an increase of the diffusion rate of these solutes due to plasma membrane permeabilization (Sá-Correia et al. 1989). Other changes were also detected in the content of the amino acids arginine and lysine. After exposure to propionic acid, the relative abundance of arginine and lysine was found to decrease during cell incubation in the presence of propionic acid. The decrease of the level of arginine during cell incubation in the presence of propionic acid is positively correlated with the decrease of ornithine. Since these two amino acids are metabolically linked, this correlation strongly suggests that their disappearance is linked.

Propionic acid-induced stress also reduced the abundance of ATP, consistent with the enrichment in genes annotated with the GO term "Generation of energy" in the set of genes required for maximal propionic acid resistance (Mira et al. 2009). The relative abundance of ATP decreased after inoculation of yeast cells into propionic acid supplemented-medium and the recovery of ATP values started during the final part of the period of growth latency when part of the viable cell population resumed duplication. ATP values in propionic acid stressed cells reached levels close to those in unstressed cells during exponential growth. To counteract intracellular acidification due to weak acid stress, the activity of the plasma membrane H^+-ATPase and of the vacuolar H^+-ATPase is stimulated (Holyoak et al. 1996; Carmelo et al. 1997;
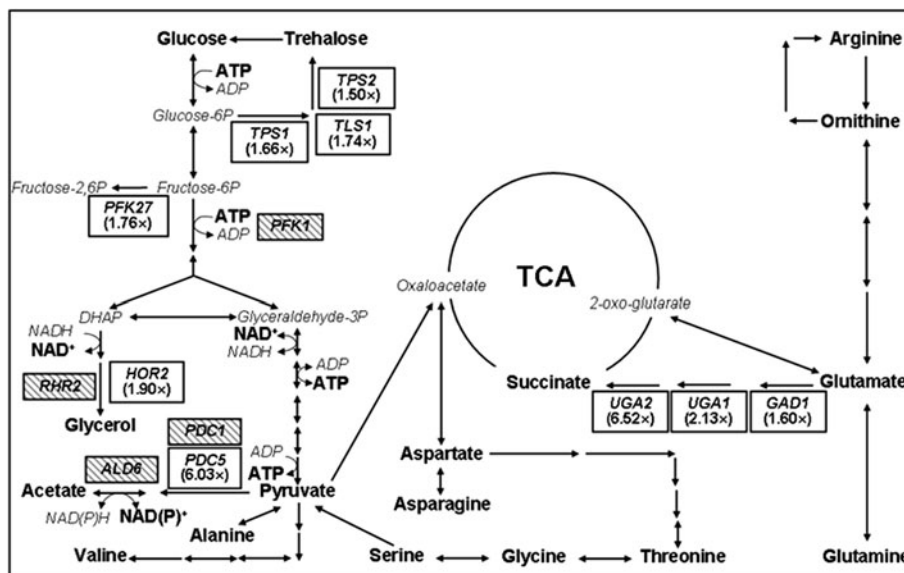
Fig. 6 Metabolic pathways involving the metabolites identified in this work as having altered content in propionic acid stressed cells. The metabolites identified in this study are in *bold*. The metabolites that are important metabolic links but not identified during this work are in *italic*. Relevant information obtained from transcriptomics and chemogenomics approaches (Mira et al. 2009) is also included in the metabolic network. The genes whose expression is altered during yeast early response to propionic acid are shown inside the *open boxes*, with the levels of differential expression shown between *brackets*. The genes whose deletion leads to propionic acid susceptibility phenotypes are shown inside the wide downward *diagonal boxes*

Viegas et al. 1998; Fernandes et al. 2003; Makrantoni et al. 2007). This adaptive response is highly energy consuming and likely involved in the initial reduction of cellular ATP levels. In *S. cerevisiae*, the ATP levels were suggested to be involved in the regulation of glycolysis based on the strong negative correlation between glycolytic flux and intracellular ATP content (Larsson et al. 1997). Our results indicate that yeast suddenly exposed to propionic acid displayed an increased level of the glycolysis end-product pyruvate, presumably due to a higher glycolytic flux. This hypothesis is consistent with the conclusions from a previous study on the response of the yeast metabolome to benzoic acid in aerobic glucose-limited chemostat cultures (Kresnowati et al. 2007). In agreement with this hypothesis is the requirement of *PDC1* expression, encoding the major isoform of the three yeast pyruvate decarboxylases, for maximal propionic acid resistance, and the up-regulation of *PDC5* encoding one of the two minor isoforms of pyruvate decarboxylase, during early response to propionic acid (Mira et al. 2009) (Fig. 6). The hypothesis of the existence of an increased glycolytic flux under propionic acid stress is further supported by the requirement of the expression of *PFK1* for maximal propionic acid resistance (Mira et al. 2009). *PFK1* encodes the alpha subunit of phosphofructokinase (Pfk1p), which is a key glycolytic enzyme (Heinisch 1986). Also supporting the importance of an increased glycolytic flux in yeast response to propionic acid is the up-regulation of *PFK27* gene during the early response to propionic acid (Mira et al. 2009). *PFK27* encodes a

6-phosphofructo-2-kinase, which catalyzes the synthesis of fructose-2,6-bisphosphate from fructose-6-phosphate and ATP (Boles et al. 1996). Fructose-2,6-bisphosphate is a strong positive allosteric effector of the glycolytic enzyme phosphofructokinase (Otto et al. 1986; Heinisch et al. 1996), and thus involved in the regulation of glycolysis. The dramatic accumulation of alanine and valine, two pyruvate-related amino acids, during propionic acid-induced lag-phase reinforces the idea of a higher glycolytic flux in response to propionic acid stress, as proposed before for other stress conditions (Devantier et al. 2005, and Pears et al. 2010). The decrease of NAD^+ during the early response to propionic acid is also a likely consequence of the hypothesized increased glycolytic flux, since the conversion of glucose to pyruvate is coupled to NAD^+ reduction. Since prolonged glycolytic activity requires the efficient regeneration of this coenzyme (Pronk et al. 1996), the intracellular accumulation of glycerol during propionic acid-induced lag-phase is likely associated to NAD^+ regeneration. The *RHR2* gene was identified as required for maximal propionic acid resistance and during the early response to propionic acid the *HOR2* gene is up-regulated (Mira et al. 2009). *RHR2* and *HOR2* code for two redundant DL-glycerol-3-phosphatases involved in glycerol biosynthesis (Fig. 6). Apart from its role in the redox balance, the accumulation of the compatible solute glycerol prevents the loss of cell turgor pressure (Blomberg and Adler 1992). Consistent with the hypothesized role of glycerol as an osmolyte in propionic acid stressed cells, both *HOG1*

and *PBS2* are required for tolerance to propionic acid (Mira et al. 2009). Trehalose is another compatible solute found to accumulate during acid-induced lag-phase, consistent with the up-regulation of trehalose biosynthetic genes (Mira et al. 2009) (Fig. 6). Trehalose is involved in yeast response to heat shock, oxidative stress and osmotic stress (Elbein et al. 2003), playing a role in *S. cerevisiae* ethanol-induced-acetic acid tolerance (Arneborg et al. 1997) and being accumulated in yeast cells exposed to sorbate (Cheng et al. 1999). The accumulation of trehalose in response to propionic acid is here described for the first time.

5 Concluding remarks

The first global study of *Saccharomyces cerevisiae* response to propionic acid stress, at the metabolome level, is presented in this article. This work highlighted the separation into two parts of the period of growth latency induced by propionic acid. The initial period is characterized by a decrease of both cell viability and average pH_i of the cell population, while during the final part of latency cell division is resumed together with an increase of the average pH_i. An association between average pH_i and the levels of both glutamate and propionate during the propionic acid-induced lag-phase was also identified, consistent with the glutamate role in the maintenance of electrical neutrality disturbed by propionate accumulation. The intracellular amino acid pools for alanine and valine showed a significant and complex dynamic alteration that is hypothesized to be related with a higher glycolytic flux during incubation in the presence of propionic acid. This response is likely a consequence of the activation of highly energy-consuming-adaptive responses to propionic acid stress. Also associated with a higher glycolytic flux are the identified changes in the abundance of NAD^+ and glycerol during propionic acid-induced lag-phase. The accumulation of the stress-responsive metabolite trehalose during propionic acid-induced lag-phase is also here described for the first time.

References

Arneborg, N., Moos, M. K., & Jakobsen, M. (1997). Induction of acetic acid tolerance and trehalose accumulation by added and produced ethanol in *Saccharomyces cerevisiae*. *Biotechnology Letters, 19*, 931–933.

Blomberg, A., & Adler, L. (1992). Physiology of osmotolerance in fungi. *Advances in Microbial Physiology, 33*, 145–212.

Boles, E., Göhlmann, H. W., & Zimmermann, F. K. (1996). Cloning of a second gene encoding 5-phosphofructo-2-kinase in yeast, and characterization of mutant strains without fructose-2, 6-bisphosphate. *Molecular Microbiology, 20*, 65–76.

Carmelo, V., Santos, H., & Sá-Correia, I. (1997). Effect of extracellular acidification on the activity of plasma membrane ATPase and on the cytosolic and vacuolar pH of *Saccharomyces cerevisiae*. *Biochimica et Biophysica Acta, 1325*, 63–70.

Cheng, L., Moghraby, J., & Piper, P. W. (1999). Weak organic acid treatment causes a trehalose accumulation in low-pH cultures of *Saccharomyces cerevisiae*, not displayed by the more preservative-resistant *Zygosaccharomyces bailii*. *FEMS Microbiology Letters, 170*, 89–95.

Cui, Q., Lewis, I. A., Hegeman, A. D., Anderson, M. E., Li, J., Schulte, C. F., et al. (2008). Metabolite identification via the Madison metabolomics consortium database. *Nature Biotechnology, 26*, 162.

de Koning, W., & Van Dam, K. (1992). A method for the determination of changes of glycolytic metabolites in yeast on a subsecond time scale using extraction at neutral pH. *Analytical Biochemistry, 204*, 118–123.

Devantier, R., Scheithauer, B., Villas-Bôas, S. G., Pedersen, S., & Olsson, L. (2005). Metabolite profiling for analysis of yeast stress response during very high gravity ethanol fermentations. *Biotechnology and Bioengineering, 90*, 703–714.

Elbein, A. D., Pan, Y. T., Pastuszak, I., & Carroll, D. (2003). New insights on trehalose: a multifunctional molecule. *Glycobiology, 13*, 17R–27R.

Fernandes, A. R., Durão, P. J., Santos, P. M., & Sá-Correia, I. (2003). Activation and significance of vacuolar H+-ATPase in Saccharomyces cerevisiae adaptation and resistance to the herbicide 2,4-dichlorophenoxyacetic acid. *Biochemical and Biophysical Research Communications, 312*, 1317–1324.

Fiehn, O. (2002). Metabolomics-the link between genotypes and phenotypes. *Plant Molecular Biology, 48*, 155–171.

Gonzalez, B., François, J., & Renaud, M. (1997). A rapid and reliable method for metabolite extraction in yeast using boiling buffered ethanol. *Yeast, 13*, 1347–1355.

Heinisch, J. (1986). Isolation and characterization of the two structural genes coding for phosphofructokinase in yeast. *Molecular Genetics and Genomics, 202*, 75–82.

Heinisch, J. J., Boles, E., & Timpel, C. (1996). A yeast phosphofructokinase insensitive to the allosteric activator fructose 2,6-bisphosphate. Glycolysis/metabolic regulation/allosteric control. *Journal of Biological Chemistry, 271*, 15928–15933.

Holyoak, C. D., Stratford, M., McMullin, Z., Cole, M. B., Crimmins, K., Brown, A. J. P., et al. (1996). Activity of the plasma membrane H+-ATPase and optimal glycolytic flux are required for rapid adaptation and growth of *Saccharomyces cerevisiae* in the presence of the weak-acid preservative sorbic acid. *Applied and Environmental Microbiology, 62*, 3158–3164.

Imai, T., & Ohno, T. (1995). The relationship between viability and intracellular pH in the yeast *Saccharomyces cerevisiae*. *Applied and Environmental Microbiology, 61*, 3604–3608.

Klionsky, D. J., Herman, P. K., & Emr, S. D. (1990). The fungal vacuole: composition, function, and biogenesis. *Microbiological Reviews, 54*, 266–292.

Krebs, H. A., Wiggins, D., Stubbs, M., Sols, A., & Bedoya, F. (1983). Studies on the mechanism of the antifungal action of benzoate. *Biochemical Journal, 214*, 657–663.

Kresnowati, M. T. A. P., van Winden, W. A., van Gulik, W. M., & Heijnen, J. J. (2007). Dynamic in vivo metabolome response of *Saccharomyces cerevisiae* to a stepwise perturbation of the ATP

requirement for benzoate export. *Biotechnology and Bioengineering, 99,* 421–441.

Larsson, C., Nilsson, A., Blomberg, A., & Gustafsson, L. (1997). Glycolytic flux is conditionally correlated with ATP concentration in *Saccharomyces cerevisiae*: a chemostat study under carbon- or nitrogen-limiting. *Conditions Journal of Bacteriology, 179,* 7243–7250.

Lundberg, P., Vogel, T., Malusek, A., Lundquist, P. O., Cohen, L., & Dahlqvist, O. (2005). *MDL—the magnetic resonance metabolomics database (mdl.imv.liu.se).* Basel, Switzerland: ESMRMB.

Makrantoni, V., Dennison, P., Stark, M. J., & Coote, P. J. (2007). A novel role for the yeast protein kinase Dbf2p in vacuolar H^+-ATPase function and sorbic acid stress tolerance. *Microbiology, 153,* 4016–4026.

Mira, N. P., Lourenço, A. B., Fernandes, A. R., Becker, J. D., & Sá-Correia, I. (2009). The RIM101 pathway has a role in *Saccharomyces cerevisiae* adaptive response and resistance to propionic acid and other weak acids. *FEMS Yeast Research, 9,* 202–216.

Mira, N. P., Teixeira, M. C., & Sá-Correia, I. (2010). Adaptive response and tolerance to weak acids in *Saccharomyces cerevisiae*: a genome-wide view. *OMICS: A Journal of Integrative Biology, 14,* 525–540.

Otto, A., Przybylski, F., Nissler, K., Schellenberger, W., & Hofmann, E. (1986). Kinetic effects of fructose-1, 6-bisphosphate on yeast phosphofructokinase. *Biomedicine Biochimica Acta, 45,* 865–875.

Pears, M. R., Codlin, S., Haines, R. L., White, I. J., Mortishire-Smith, R. J., Mole, S. E., et al. (2010). Deletion of *btn1*, an orthologue of *CLN3*, increases glycolysis and perturbs amino acid metabolism in the fission yeast model of Batten disease. *Molecular BioSystems, 6,* 1093–1102.

Piper, P., Mahé, Y., Thompson, S., Pandjaitan, R., Holyoak, C., Egner, R., et al. (1998). The Pdr12 ABC transporter is required for the development of weak organic acid resistance in yeast. *EMBO Journal, 17,* 4257–4265.

Piper, P., Ortiz-Calderon, C., Hatzixanthis, K., & Mollapour, R. M. (2001). Weak acid adaptation: the stress response that confers yeasts with resistance to organic acid food preservatives. *Microbiology, 147,* 2635–2642.

Pronk, J. T., van der Linden-Beuman, A., Verduyn, C., Scheffers, W. A., & van Dijken, J. P. (1994). Propionate metabolism in *Saccharomyces cerevisiae*: implications for the metabolon hypothesis. *Microbiology, 140,* 717–722.

Pronk, J. T., Yde Steensma, H., & Van Dijken, J. P. (1996). Pyruvate metabolism in *Saccharomyces cerevisiae*. *Yeast, 12,* 1607–1633.

Roberts, C. J., Raymond, C. K., Yamashiro, K. T., & Stevens, T. H. (1991). Methods for studying the yeast vacuole. *Methods in Enzymology, 194,* 644–661.

Roe, A. J., Mclaggan, D., Davidson, I., O'Byrne, C., & Booth, I. R. (1995). Perturbation of anion balance during inhibition of growth of *Escherichia coli* by weak acids. *Journal of Bacteriology, 180,* 767–772.

Sá-Correia, I., Dos Santos, S. C., Teixeira, M. C., Cabrito, T. R., & Mira, N. P. (2009). Drug:H^+ antiporters in chemical stress response in yeast. *Trends in Microbiology, 17,* 22–31.

Sá-Correia, I., Salgueiro, S. P., Viegas, C. A., & Novais, J. M. (1989). Leakage induced by ethanol, octanoic and decanoic acids in *Saccharomyces cerevisiae*. *Yeast, Special Issue, 5,* S123–S127.

Suhr, K. I., & Nielsen, P. V. (2004). Effect of weak acid preservatives on growth of bakery product spoilage fungi at different water activities and pH values. *International Journal of Food Microbiology, 95,* 67–78.

Teixeira, M. C., Duque, P., & Sá-Correia, I. (2007). Environmental genomics: mechanistic insights into toxicity of and resistance to the herbicide 2,4-D. *Trends in Biotechnology, 25,* 363–370.

Viegas, A. C., Almeida, P. F., Cavaco, M., & Sá-Correia, I. (1998). The H^+-ATPase in the plasma membrane of *Saccharomyces cerevisiae* is activated during growth latency in octanoic acid-supplemented medium accompanying the decrease in intracellular pH and cell viability. *Applied and Environmental Microbiology, 64,* 779–783.

Viegas, A. C., & Sá-Correia, I. (1995). Toxicity of octanoic acid in *Saccharomyces cerevisiae* at temperatures between 8.5 and 30°C. *Enzyme and Microbial Technology, 17,* 826–831.

Vindelov, J., & Arneborg, N. (2002). *Saccharomyces cerevisiae* and *Zygosaccharomyces mellis* exhibit different hyperosmotic shock responses. *Yeast, 19,* 429–439.

Westerhuis, J. A., Kourti, T., & MacGregor, J. F. (1999). Comparing alternative approaches for multivariate statistical analysis of batch process data. *Journal of Chemometrics, 13,* 397–413.

Wishart, D. S., Knox, C., Guo, A. C., Eisner, R., Young, N., Gautam, B., et al. (2009). HMDB: a knowledgebase for the human metabolome. *Nucleic Acids Research, 37,* D603–D610.